International Journal of Engineering

Journal Homepage: www.ije.ir

Refractive Index Perception and Prediction of Radio wave through Recursive Neural Networks using Meteorological Data Parameters

S. Adebayo[a], F. O. Aweda*[b], I. A. Ojedokun[c], O. T. Olapade[b]

[a] *Mechatronics Engineering Programme, College of Agriculture, Engineering, and Science, Bowen University, Iwo, Osun State, Nigeria*
[b] *Physics and Solar Energy Programme, College of Agriculture, Engineering, and Science, Bowen University, Iwo, Osun State, Nigeria*
[c] *Electrical and Electronics Department, Federal University, Otuoke, Nigeria*

PAPER INFO

Paper history:
Received 26 August 2021
Received in revised form 02 November 2021
Accepted 23 December 2021

Keywords:
Radio Refractivity
Meteorological Data
International Telecommunication Union
Long-Short Term Memory
Wireless Communication

ABSTRACT

Radio refractivity is very crucial in the optimal performance of radio systems and is one of the attributes that affect electromagnetic waves in the troposphere. This study presented a comparison of different variants of recurrent neural networks to predict radio refractivity index. The radio refractivity index is predicted based on forty-one years (1980 to 2020) metrological data obtained from the MERRA-2 data re-analysis database. The refractivity index was computed using International Telecommunication Union (ITU) standard. The correlation refractivity index was categorized into strong, weak and no correlation. Rainfall, relative humidity, and air pressure fall in the first category, the temperature falls in the second category while wind speed falls in the last one. The true future and predicted values of the radio refractivity index are close with GRU performing better than the other two models (LSTM and BiLSTM) which proves the accuracy of the proposed model. In conclusion, the proposed model can establish a radio refractivity status of locations at different times of the season, which is of great importance in the effective design, development, and deployment of radio communication systems.

***doi**: 10.5829/ije.2022.35.04a.21*

1. INTRODUCTION

Wireless communication (WC) is the transmission of information from the source to the destination without a physical connection. The channel of propagation of signals is the atmosphere which consist of three layers: troposphere, stratosphere, and ionosphere. The troposphere and ionospheric possess challenges ranging from scattering, absorption, obstruction and so on which cause severe impairment on the received signal. In the troposphere, there is the presence of some meteorological parameters such as temperature, relative humidity and pressure which varies in quantity per time and are responsible for radio signal disorientation and consequently, corruption of the transmitted signals. Radiowave [1] is one of the components of the electromagnetic spectrum and a means of signal propagation in the WC channel. It was first discovered by a Scottish Mathematician James Clerk Maxwell in the mid- 1860. The prediction of Maxwell was verified in the laboratory by Marconi in 1899 [2]. Radio waves are electromagnetic radiation with a wavelength falling between 3cm and 30km and frequency is between 3kHz and 3GH. Radio waves travel at the speed of light and thus enhances the speed at which information is received. Waves are characterized by reflection, interference, diffraction, absorption, scattering, and refraction. The heterogeneous nature of the tropospheric layers, due to the presence of meteorological parameters enhances large scale variation in the signal strength and direction [3]. Consequently, rapid fluctuation of the signal over some time and distance occurs. Other physical impairments suffered by WC in a refracted channel include sub-refraction, super refraction and ducting and these impairments cause performance degradation and drop calls at the receiving end [4]. Several researchers have

*Corresponding Author Institutional Email: *aweda.francis@bowen.edu.ng* (F. O. Aweda)

Please cite this article as: S. Adebayo, F. O. Aweda, I. A. Ojedokun, O. T. Olapade, Refractive Index Perception and Prediction of Radio wave through Recursive Neural Networks using Meteorological Data Parameters, ***International Journal of Engineering, Transactions A: Basics*** Vol. 35, No. 04, (2022) 810-818

resulted in taking measurements of metrological data in the troposphere during wet and dry seasons within a certain period. These measurements were taken to study the trend of the effect of these parameters on the received signal. Consequently, the refractive nature of the WC channel can be observed and necessary action by network designers and operators could be taken to ameliorate the effect of the refractive nature of the troposphere. To overcome the challenges in measurement taken for estimating the radio refractivity and refractivity gradient, which could be because of human and equipment error, this research, therefore, focuses on developing a model using a machine learning approach. Machine Learning (ML) is a process of developing a machine that will enable it to learn without programming the machine explicitly [5]. ML process includes data collection of historical meteorological data, data preprocessing the data, features extraction, algorithm training, model evaluation, and model deployment. The focus of this work is to create a reliable platform on metrological data perception as well as predicting radio refractivity index for the communication design process. Due to the challenges faced by engineers, researchers and designers of wireless communication systems, this work presents a suitable recurrent neural network model for predicting radio refractivity index using different meteorological parameters. This model will help during the condition of the ducts by hidden from sight in residential and commercial buildings, and performance issues that may stay undetected. Thus, for effective propagation of radio waves through the atmosphere, there is a need to continuously understudy the variation of these parameters over some time and the result thoroughly analyzed to aid the planning of network providers in rendering quality services to their customers [6]. Gao et al. [7] examined the effect of moisture and temperature on radio refractivity and its influence on radar ray path. Analysis of the different radio refractivity concerning atmospheric temperature and moisture was done. The results showed that moisture gradient is a significant contributor to radio refractivity gradient at the lower troposphere. Hence, moisture has a more significant influence on the radar ray path calculations than temperature. Adediji et al. [8] looked at the radio refractivity gradient and its effect on the earth radius factor (k factor) over Akure, Southwestern Nigeria. Okoro and Agbo [9], Oluwole [10] worked on Meteorological Parameters and the effect on tropospheric radio refractivity for Akure South –West, and in Minna north central Nigeria. Oluwole [10] reported that the variation in radio wave propagation in Akure is because of changes in temperature, pressure, and humidity. However, Data for the daily intervals of these parameters in the troposphere for Akure were obtained from Nigeria Meteorological Agency (NIMET) for the year 2013. The result revealed that Akure has the lowest radio refractivity in January (dry season) the highest radio refractivity in August (wet season) due to an increase in the humidity and temperature in the troposphere. The model used is not a predictive one and it was used to capture only Akure. Study by Amajama [11] established a mathematical relationship between radio refractivity and its meteorological components with a new mathematical equation to determine radio refractivity. The study revealed the correlations between radio refractivity and metrological parameters which was given as atmospheric temperature: 0.99; atmospheric pressure: 0.91; and relative humidity: 0.99. Zhang et al. [12] evaluate the performance of different machine-learning-based models in comparison to the empirical model for the prediction of radio signal path loss. It was concluded that machine-learning-based models perform better in terms of prediction accuracy and computational efficiency than the empirical model. However, the research is not in any way related to the propagation condition of radio signals in southwestern Nigeria. Neural Networks had been used in predicting metrological parameters for certain regions such as Pakistan [13] and West Java [14]. Applying neural networks to metrological data in Nigeria will help in gaining useful insight. Thus, this research aims to bridge the gaps in knowledge by developing a radio refractivity predictive model using long-short term memory (LSTM), Bi long-short term memory (BiLSTM) and Gated Recurrent Unit (GRU) neural network.

2. ARTIFICIAL NEURAL NETWORK

An artificial neural network is a machine learning process that uses a similar principle of operation to the working operation of a human brain. The neural networks used in deep learning consists of several layers connected. The network learns from a massive volume of data and uses algorithms to train a neural network. There are several popular neural networks which include a feed-forward neural network [15] which is used in general regression and classification problems. Convolutional neural network (CNN) is generally used for image recognition [16], deep neural network (DNN) is for acoustic modelling [17]. A deep belief network (DBN) has been used for cancerous cell detection [18] while a recurrent neural network (RNN) is generally used in speech recognition [19].

2. 1. Recurrent Neural Network (RNN) In feed-forward network, information flow in the forward direction from the input nodes without loops or cycle in the network. Decisions are based on the current input without memory of the past and future. FFN is greatly impaired by the inability to handle sequence data because; it does not have a scope of memory or time.

RNN is an improved feed-forward network that allows previous outputs to be used as inputs. The internal state (memory) in RNN is used to process sequences of inputs. This network architecture has been applied in natural language processing problems [20] such as text mining, sentiment analysis and machine translation. The network can be represented mathematically as:
For the given hidden layers, the new state is given as:

$$h_{(t)} = f_c\left(h_{(t-1)}, x_{(t)}\right) \quad (1)$$

where f_c is the function with c parameter, $h(t-1)$ is the previous state and $x(t)$ is the input vector at time step t. Applying activation function gives:

$$h_{(t)} = tanh\left(W_{hh}h_{(t-1)} + W_{xh}x_{(t)}\right) \quad (2)$$

and the output state is given as:

$$y_{(t)} = W_{hy}h_{(t)} \quad (3)$$

W is the input weight**,** h is the hidden vector for a single neuron, W_{hh} ***is*** the previous weight, W_{hx} *is* the weight at the current input state, and tanh is the activation function**.** RNN structure can be classified into four categories: multiple-input, multiple-output (MIMO), single-input, single-output (SISO), single-input, multiple-outputs (SIMO) and multiple-input, single-output (MISO). RNN is greatly affected by the problems of vanishing and exploding gradient. This makes RNN training a very difficult task. There is also a limitation on the length of sequence data it can process when singing hyperbolic tangent function (tanh) or Rectified Linear Unit (ReLu) activation function. Thus, the need for better variants of this network architecture.

2. 2. Long-Short Time Memory (LSTM) Network Architecture Long Short-Term Memory (LSTM) network was developed to address the problem of the RNN which is the vanishing gradient problem. LSTM is capable of processing and predicts time series data. This is achieved using the back-propagation method. The architecture of the LSTM network consists of three gates:

1. Input gate. This gate determines the values to go through using a sigmoid function while the tanh function determines the level of importance of the value through weights. This weight ranges from -1 to 1 as represented in equation:

$$i_t = \sigma(W_i[h_{t-1}, x_t] + b_i) \quad (4)$$

$$c_t = tanh(W_c[h_{t-1}, x_t] + b_c) \quad (5)$$

2. Forget gate decide, using the sigmoid function, input values to be discarded from the network. This is done by examining the values of the previous state (h_{t-1}), the input (x_t) and outputs for each number in the cell state (C_{t-1}). When the value is 0, the value is omitted while the value 1 is kept. The forget gate is represented in Equation (6):

$$f_t = \sigma\left(W_f[h_{t-1}, x_t] + b_f\right) \quad (6)$$

3. The gate in this architecture is the output gate. This gate has a sigmoid function which decides the values to let through either 0 or 1. The tanh function in this gate gives weights to the values which reflect the level of importance. The final out is further multiplied with the output of a sigmoid function.

$$o_t = \sigma(W_o[h_{t-1}, x_t] + b_o) \quad (7)$$

$$h_t = o_t * tanh(c_t) \quad (8)$$

Gated Recurrent Unit (GRU)
GRU is another variant of Recurrent Neural networks with similar architecture as LSTM. The cell state is replaced with a hidden state in the transfer of information. Furthermore, unlike the LSTM with three gates, GRU has two gates: a reset gate and an update gate. The update gate is like the forget and input gate in an LSTM. This gate determines the type of information to discard or accept. The reset gate is used to decide the level of past information to forget. it has been shown that due to fewer operations in GRU, the training time is shorter than LSTM.
The reset gate is given as:

$$r_t = \sigma(W^{(ir)}\bar{x}_t + W^{(hr)}h_{t-1} \quad (9)$$

The updated gate is given as:

$$z_t = \sigma(W^{(iz)}\bar{x}_t + W^{(hz)}h_{t-1} \quad (10)$$

The process input is given as:

$$\tilde{h}_t = \tanh(W^{(i\tilde{h})}\bar{x}_t + W^{(h\tilde{h})}h_{t-1} \quad (11)$$

The hidden state update is given as:

$$h_t = (1 - z_t) * h_{t-1} + z_t * \tilde{h}_t \quad (12)$$

And the output is given as:

$$y_t = h_t \quad (13)$$

3. METHODOLOGY

3. 1. Proposed Model The research work involves the collection of data from meteorological database parameters. The dataset was analyzed by clustering to gain insight into data and to help data simplification which may be needed before further processing. Neural networks extract relevant features from the dataset for training to predict the radio refractivity index of an environment. The model was compared with other statistical developed models for evaluation and validation. The performance of the proposed model was further evaluated on some selected metrics such as Mean Average Error (MAE), Root Mean Square Error (RMSE) and R square.

3. 2. Study Area The stations used for this research consists of the following Abuja, Awka, Calabar, Enugu, Ibadan, Ikeja, Ilorin, Kaduna, Maiduguri, Port Harcourt, Sokoto and Yola. These stations were selected across the entire country (see Table 1).

These stations are divided into different climatic areas to show the effect of radio transmission across the entire country. Figure 1 shows the station presents in Nigeria.

Figure 1. Map showing selected stations across Nigeria

TABLE 1. The coordinate of the stations used

Stations	Longitude ^{0}N	Latitude ^{0}E
Abuja	9.0723	7.4913
Awka	6.2105	7.0722
Calabar	4.9828	8.3345
Enugu	6.4599	7.5489
Ibadan	7.4020	3.9173
Ikeja	6.6059	3.3491
Ilorin	8.5000	4.5500
Kaduna	10.6093	7.4295
Maiduguri	11.8333	13.1500
Port Harcourt	4. 7774	17.0134
Sokoto	13.0058	5.2475
Yola	9.2035	12.1495

3. 4. Data Collection The data used in this study consists of monthly rainfall, air temperature, water vapour, pressure, relative humidity, wind speed and direction for twelve stations which were obtained from the archive of the HelioClim website of soda (http://www.soda-pro.com) of MERRA-2 meteorological re-analysis data as recommended by Gelaro et al. [21]. The assessment of the data was on 22nd August 2020. The data of forty-one years spanning from 1980 to 2020 were obtained as a monthly average for January to December of every year in comma-separated value (CSV) data format.

3. 3. Dataset Preprocessing Radio refractivity and radio refractive index data were computed using the formula provided by the Radio communication sector of the International Telecommunication Union (ITU-R). ITU-R is saddle with the responsibility of ensuring efficient and economical use of the radiofrequency spectrum by all radio communication services. This is done by the provision of radio refractive index, n, and is computed by Equation (14):

TABLE 2. Selected Metrological Dataset for Ibadan Station

Date	Station	Temp. (K)	RH (%)	Pressure (hPa)	Rainfall (kg/m^2)	Wind Speed (m/s)	Wind direction (deg)	Refractivity Index
1980-01-31	Ibadan	298.56	78.48	990.22	43.64	1.33	219.77	2576.23
1980-02-28	Ibadan	299.05	78.77	988.83	68.55	1.71	219.13	2576.34
1980-03-31	Ibadan	299.27	81.01	989.22	105.14	2.35	213.82	2645.25
1980-04-30	Ibadan	299.09	83.47	989.43	90.25	2.48	214.60	2729.19
1980-05-31	Ibadan	298.40	86.54	991.07	151.17	2.19	220.69	2844.09

$$n = 1 + N \times 10^{-6} \quad (14)$$

The radio refractivity, N, is given as:

$$N = 77.6\frac{P_d}{T} + 72\frac{e}{T} + 3.75\times 10^5 \frac{e}{T^2} \quad (15)$$

where the dry component of the radio refractivity, N_{dry} is given as:

$$N_{dry} = 77.6\frac{P_d}{T} \quad (16)$$

and the wet component, N_{wet} is:

$$N_{wet} = 72\frac{e}{T} + 3.75\times 10^5 \frac{e}{T^2} \quad (17)$$

P_d and P is the dry and total atmospheric pressure respectively, while e is the water vapour pressure all in (hPa). T is the absolute temperature given in Kelvin. Since $P_d = P - e$, Equation (1) can be rewritten as:

$$N = 77.6\frac{P}{T} + 72\frac{e}{T} + 3.75\times 10^5 \frac{e}{T^2} \quad (18)$$

The relationship between water vapour pressure e and relative humidity is given as follows:

$$e = \frac{H.e_s}{100} \quad (19)$$

$$e_s = EF.a.exp\left[\frac{\left(b-\frac{t}{d}\right).t}{t+c}\right] \quad (20)$$

$$EF_{water} = 1 + 10^{-4}[7.2 + P.(0.00320 + 5.9\times10^{-7}.t^2)] \quad (21)$$

$$EF_{ice} = 1 + 10^{-4}[2.2 + P.(0.00382 + 6.4\times10^{-7}.t^2)] \quad (22)$$

where t: temperature (°C), P: pressure (hPa), H: relative humidity (%), e_s: saturation vapour pressure (hPa) at the temperature t (°C) and the coefficients a, b, c, and d are:
for water: a = 6.1121, b = 18.678, c = 257.14, d = 234.5. This is valid between -40 and +50°
for ice: a = 6.1115, b = 23.036, c = 279.82, d = 333.7. This is valid between -80° and 0° [6].

3. 5. Evaluation Metrics The developed model was evaluated using the following statistical methods:
1. Mean Average Error (MAE): this is given in equation:

$$MAE = \frac{\sum_{i=1}^{n}|m_i - p_i|}{n} \quad (23)$$

2. Root mean square error which is given in the equation

$$RMSE = \sqrt{\frac{\sum_{i=1}^{n}(m_i - p_i)^2}{n}} \quad (24)$$

R squared is given as:

$$R^2 = \frac{(\sum_{i=1}^{n}(P_i - \bar{P})\,(P'_i - \bar{P}'))^2}{\sum_{i=1}^{n}(P_i - \bar{P})^2 \sum_{i=1}^{n}(P'_i - \bar{P}')^2} \quad (25)$$

where P_i is the observed data, P'_i is the simulated data, $\bar{P}$ is the mean of the observed data, $\bar{P}'$ is the mean of the simulated data and e is the model error. Where m_i is the prediction data while p_i pi is the observed data, n is the number of errors

3. 6. Open-source Tools The research relied heavily on open-source software. Python 3.8 was the chosen programming language that has the capability of importing libraries such as Numpy, Pandas, and Sckit-Learn for data preprocessing and data management. TensorFlow [22] and Keras [23] provided the framework for training the algorithms. Matplotlib [24] library helped in creating figures and graphs.

4. RESULTS AND DISCUSSION

4. 1. Data Visualization The effect of environmental parameters on the refractivity of a radio waves can be grouped into three categories from Figure 2(a) to 2(f). This is categorized as follows:
1. Weak Correlation: Figure 2(a) shows the correlation between refractivity and temperature. The effect of the increase in temperature on radio refractivity is not apparent, although the temperature was at its highest in February before it started falling to rise again in November. It can be deduced that the effect of temperature contributes little to variation of radio refractivity index in this region as proven by [25].
2. Strong Correlation: Figures 2(b), 2(c) and 2(d) are plots of refractivity against rainfall, relative humidity, and pressure respectively. The result revealed a strong correlation between each of these features and radio refractivity. It can be seen, from Figure 2(b), that as the rainfall increases, the radio waves refractivity increases as well for the number of years considered. The Result from Figures 2(b), 2(c) and 2(d) agree with several studies [25, 26].
3. No Correlation: The relationship between wind speed, wind direction and refractivity does not show any correlation as shown in Figures 2(e) and 2(f).

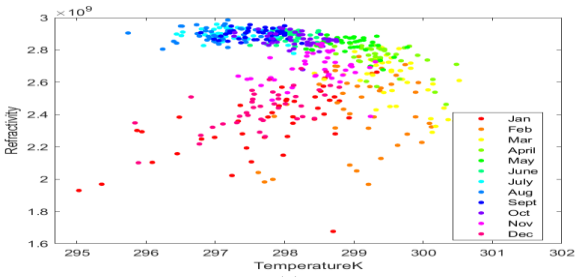

(a)

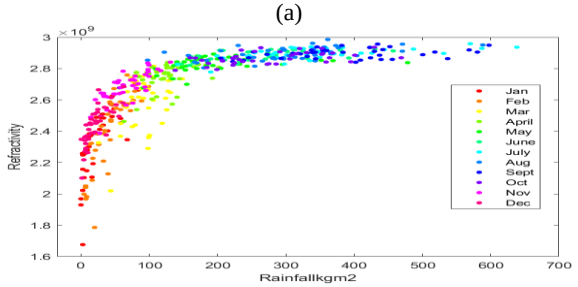

(b)

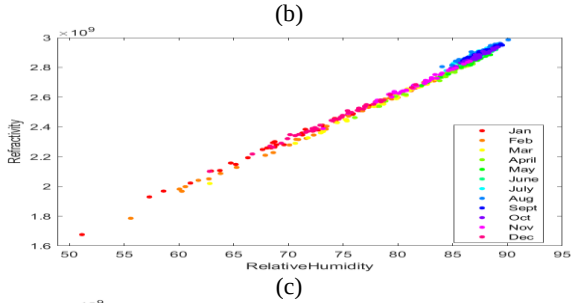

(c)

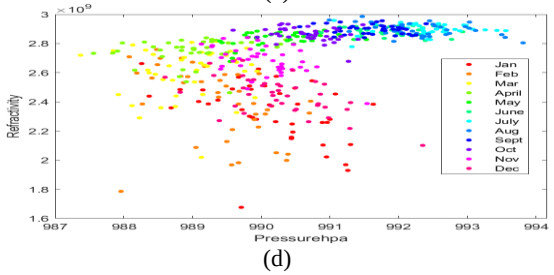

(d)

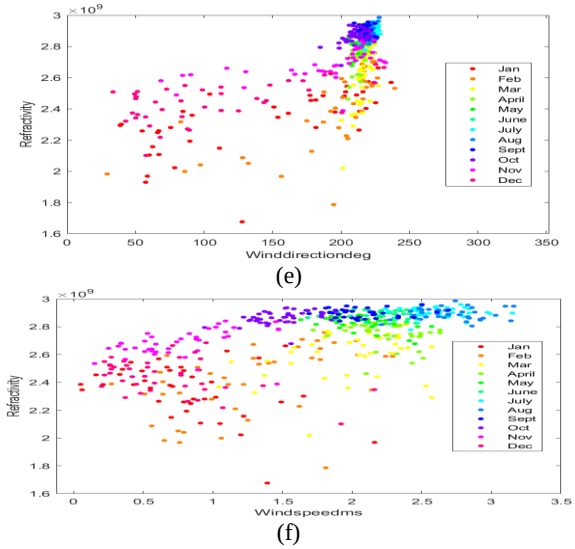

Figure 2. Explanatory Data Analysis of the refractivity against various metrological parameters

4. 2. Dataset Distribution Pattern The metrological dataset for the considered location is presented in Table 3. The 491-dataset span over 41 years. The minimum and maximum temperatures are 295.03K and 301.39K respectively. The relative humidity, within these years, ranges between 51.13 and 90.06 while the atmospheric pressure is between 987.37 and 993.81. The rainfall is at its lowest mostly in December or January, while it is at its highest in July. The rainfall minimum and maximum datasets are between 0.01 and 638.32. The radio refractivity index values fall between 1677.02 and 2986.68.

4. 3. Training and Test Dataset Figure 3 shows the split ratio of the dataset into train and test sets. 80% of the dataset was set for the training set while the remaining 20% was used for the test set. The training dataset span from 1980 to 2012 while the test dataset is from 2013 to 2020.

TABLE 3. Descriptive statistics of the measured meteorological data for input to RNN

Statistical Parameter	T (K)	RH (%)	P (hPa)	RF (mm)	Refractivity Index
Count	491.000000	491.000000	491.000000	491.000000	491.000000
Mean	298.260061	82.325336	990.575112	178.840035	2708.644544
Std	0.974740	7.045053	1.311667	141.762511	234.514598
Min	295.030000	51.130000	987.370000	0.010744	1677.023932
25%	297.590000	78.725000	989.600000	57.609324	2578.606102
50%	298.200000	85.710000	990.470000	141.306552	2809.317710
75%	298.995000	87.370000	991.620000	285.793902	2882.642596
Max	301.390000	90.060000	993.810000	638.320680	2986.682195

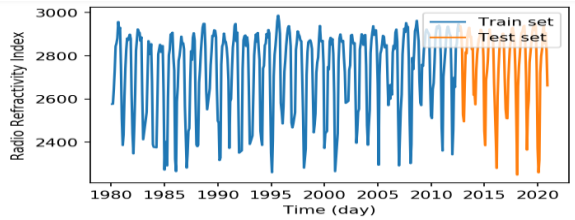

Figure 3. Train and test set split ratio of 4 to 1

4. 4. Performance of the Training Algorithm Table 4. Shows the performance of LSTM, BiLSTM and GRU models based on three evaluation metrics: R2, MAE and RMSE. The architecture of the models is greatly determined by the neurons in the hidden layers as well as the hyper-parameter turning. To obtain the optimal architecture, the hidden layers were varied from two to five, with each layer containing thirty neurons. The coefficient of determination (R^2) for LSTM, BiLSTM and GRU with 2 layers is 0.84, 0.79, 0.87. This shows that the GRU model performs better. Furthermore, the performance of the model reduces as the complexity of the model increases. R^2 value reduces from 0.87 to 0.71 when the layers of the network were increased from 2 to 5. The MAE and RMSE values reveal that with an increase in neurons, GRU and BiLSTM tend to marginally minimize prediction errors in comparison with the LSTM neural network model. GRU outperformed both the BiLSTM and LSTM with just a marginal gap. Table 4 also shows that the MAE and RMSE in radio refractivity index prediction using GRU with one hidden layer has the lowest error.

Furthermore, the difference in the performance of LSTM, BiLSTM and GRU in radio refractivity index prediction in terms of training and validation loss is presented in Figure 3. The minimum training and validation cost (loss) functions are 0.0105 and 0.0145 at epoch 87th for BiLSTM, 0.0156 and 0.0160 at 73rd for LSTM and 0.0153 and 0.0112 at epoch 67th for GRU. This shows that the GRU model has a faster convergence

time, although BiLSTM has the lowest cost function. The training process was stopped when the validation error trend changes from descending to ascending to avoid model overfitting.

Figure 4 shows the radio refractivity index predictions for the 3 trained models using 20% of the dataset (test set). All the models performed well because the predicted values are very close to the true future values (see Figure 5).

Bazoobandi [27] stated that a wavelet neural network has two types of parameters, namely wavelet function parameters (translation, dilation) and the weights between the hidden layer and output layer.

TABLE 4. Performance of radio refractivity index prediction for different RNN variants using statistical metrics

Hidden Layer	LSTM			BILSTM			GRU		
	MAE (unit)	RMSE	R^2	MAE (unit)	RMSE	R^2	MAE (unit)	RMSE	R^2
2	57.08	74.75	0.84	53.07	86.12	0.79	51.10	67.78	0.87
3	60.25	78.45	0.83	53.11	86.34	0.79	52.68	67.85	0.87
4	59.17	97.74	0.73	54.02	87.37	0.79	71.03	85.83	0.79
5	60.93	85.98	0.79	67.92	92.29	0.76	80.54	100.77	0.71

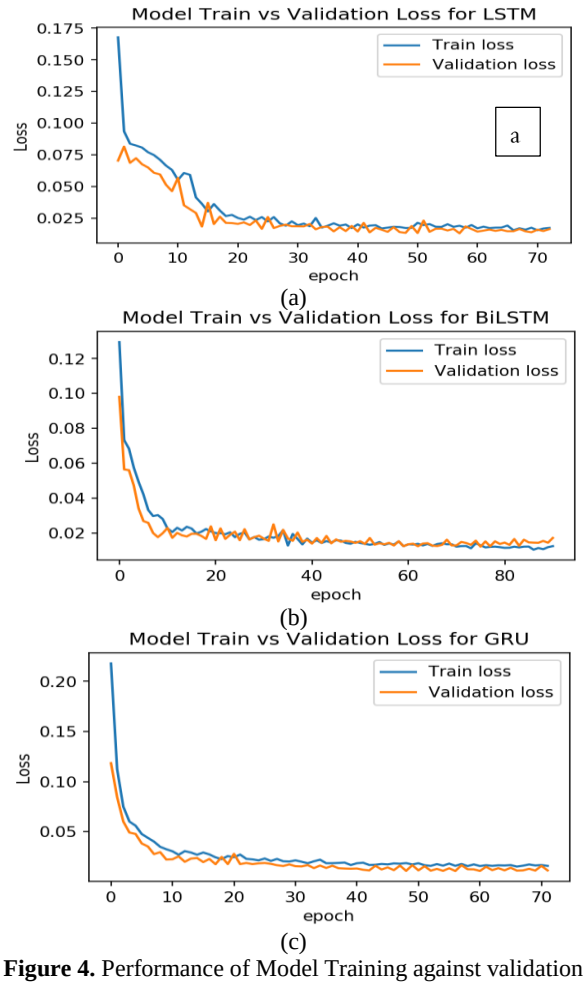

Figure 4. Performance of Model Training against validation Loss

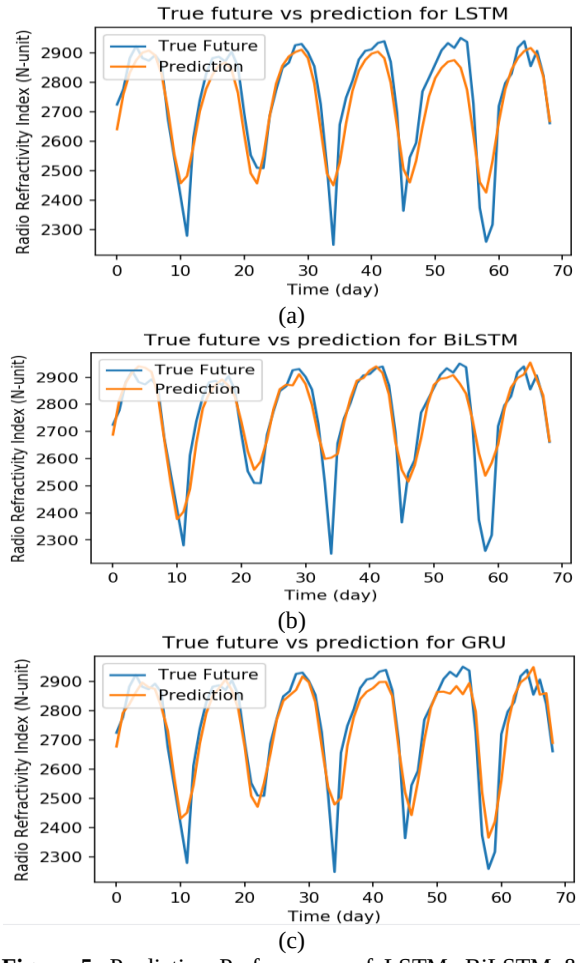

Figure 5. Prediction Performance of LSTM, BiLSTM & GRU

5. CONCLUSION

Radio refractivity is an important feature in the behavioral patterns of electromagnetic waves, which translate to the performance of the communication systems. The focus of this study is to present a comparison of different variants of recurrent neural networks to predict radio refractivity index. The radio refractivity index was predicted based on forty-one years (1980-2020) metrological data. These data are categorized as temperature, pressure relative humidity and rainfall, and they were obtained from the website of Solar Radiation Data (SoDa) database. The refractivity index was computed using International Telecommunication Union (ITU) standard. The data were analyzed through the explanatory data analysis (EDA) method for better perception. Long- and short-term memory (LSTM), Bi-Long- and short-term Memory (BiLSTM) and Gated Recurrent Unit (GRU) neural networks were trained to learn features from the dataset. The refractivity index for the year 2021 was predicted based on the knowledge learned from the previous forty-one years. The trained model's predictions and estimation were validated against each other. The correlation of the features considered concerning the radio refractivity index was categorized into strong, weak and no correlation. Rainfall, relative humidity, and pressure fall in the first category, the temperature falls in the second category while wind speed falls in the last. The true future and predicted values of the radio refractivity index are close with GRU performing better than the other two models (LSTM and BiLSTM) which proves the accuracy of the proposed model. The proposed model can establish a radio refractivity status of locations at different times of the season, which is of great importance in the effective design, development, and deployment of radio communication systems. Therefore, this research recommends to the government of the Federal Republic of Nigeria, to create research centres for data collection and analysis.

6. REFERENCES

1. Sizun, H. and de Fornel, P., "Radio wave propagation for telecommunication applications, Springer, (2005). http://www.eletrica.ufpr.br/armando/index_arquivos/Radio%20Wave%20Propagation.pdf
2. Erceg, V., Greenstein, L.J., Tjandra, S.Y., Parkoff, S.R., Gupta, A., Kulic, B., Julius, A.A. and Bianchi, R.J.I.J.o.s.a.i.c., "An empirically based path loss model for wireless channels in suburban environments", Vol. 17, No. 7, (1999), 1205-1211, doi: 10.1109/49.778178.
3. Seybold, J.J.I., Hoboken, New Jersey, "Introduction to rf propagation. John wiley & sons", (2005), doi: 10.1002/0471743690.
4. Dinc, E. and Akan, O.B.J.I.c.m., "Beyond-line-of-sight communications with ducting layer", Vol. 52, No. 10, (2014), 37-43.
5. Mohammed, M., Khan, M.B. and Bashier, E.B.M., "Machine learning: Algorithms and applications, Crc Press, (2016). https://doi.org/10.1201/9781315371658
6. Boano, C.A., Tsiftes, N., Voigt, T., Brown, J. and Roedig, U.J.I.T.o.I.I., "The impact of temperature on outdoor industrial sensornet applications", Vol. 6, No. 3, (2009), 451-459, doi: 10.1109/TII.2009.2035111.
7. Gao, J., Brewster, K. and Xue, M., "Variation of radio refractivity with respect to moisture and temperature and influence on radar ray path", ***Advances in Atmospheric Sciences***, Vol. 25, No. 6, (2008), 1098-1106.
8. Adediji, A., Ajewole, M. and Falodun, S., "Distribution of radio refractivity gradient and effective earth radius factor (k-factor) over akure, south western nigeria", ***Journal of Atmospheric and solar-Terrestrial Physics***, Vol. 73, No. 16, (2011), 2300-2304.
9. Okoro, O. and Agbo, G.J.G.J.o.s.F.r., "The effect of variation of meteorological parameters on the tropospheric radio refractivity for minna", Vol. 12, (2012), 37-41.
10. Oluwole, F.J., "Variation of metrological parameters as they affect the tropospheric radio refractivity for akure south-west nigeria", ***International Journal of Environment***, Vol. 7, No. 10, (2013), 458-460.
11. Amajama, J., "Mathematical relationships between radio refractivity and its meteorological components with a new linear mathematical equation to determine radio refractivity", ***International Journal of Innovative Science, Engineering & Technology***, Vol. 2, No. 12, (2015), 953-957.
12. Zhang, Y., Wen, J., Yang, G., He, Z. and Wang, J., "Path loss prediction based on machine learning: Principle, method, and data expansion", ***Applied Sciences***, Vol. 9, No. 9, (2019), 1908.
13. Javeed, S., Alimgeer, K.S., Javed, W., Atif, M. and Uddin, M., "A modified artificial neural network based prediction technique for tropospheric radio refractivity", ***Plos One***, Vol. 13, No. 3, (2018), e0192069.
14. Priatna, M.A. and Djamal, E.C., "Precipitation prediction using recurrent neural networks and long short-term memory", ***Telkomnika***, Vol. 18, No. 5, (2020), 2525-2532.
15. Fine, T.L., "Feedforward neural network methodology, Springer Science & Business Media, (2006).
16. Albawi, S., Mohammed, T.A. and Al-Zawi, S., "Understanding of a convolutional neural network", in 2017 international conference on engineering and technology (ICET), IEEE. (2017), 1-6.
17. Yangzhou, J., Ma, Z. and Huang, X., "A deep neural network approach to acoustic source localization in a shallow water tank experiment", ***The Journal of the Acoustical Society of America***, Vol. 146, No. 6, (2019), 4802-4811.
18. Ronoud, S. and Asadi, S., "An evolutionary deep belief network extreme learning-based for breast cancer diagnosis", ***Soft Computing***, Vol. 23, No. 24, (2019), 13139-13159.
19. Amberkar, A., Awasarmol, P., Deshmukh, G. and Dave, P., "Speech recognition using recurrent neural networks", in 2018 international conference on current trends towards converging technologies (ICCTCT), IEEE. (2018), 1-4. https://doi.org/10.1007/s10772-021-09808-0
20. Yin, W., Kann, K., Yu, M. and Schütze, H., "Comparative study of cnn and rnn for natural language processing", arXiv preprint arXiv:1702.01923, (2017).
21. Gelaro, R., McCarty, W., Suárez, M.J., Todling, R., Molod, A., Takacs, L., Randles, C.A., Darmenov, A., Bosilovich, M.G. and Reichle, R.J.J.o.c., "The modern-era retrospective analysis for research and applications, version 2 (merra-2)", Vol. 30, No. 14, (2017), 5419-5454.
22. Abadi, M., Agarwal, A., Barham, P., Brevdo, E., Chen, Z., Citro, C., Corrado, G.S., Davis, A., Dean, J. and Devin, M., "Tensorflow:

Large-scale machine learning on heterogeneous distributed systems. Arxiv 2016", arXiv preprint arXiv:1603.04467, (2019).

23. Gulli, A. and Pal, S., "Deep learning with keras, Packt Publishing Ltd, (2017). https://www.packtpub.com/product/deep-learning-with-keras/9781787128422
24. Bisong, E., Matplotlib and seaborn, in Building machine learning and deep learning models on google cloud platform. 2019, Springer.151-165.
25. Agbo, E., Ettah, E. and Eno, E., "The impacts of meteorological parameters on the seasonal, monthly, and annual variation of radio refractivity", ***Indian Journal of Physics***, (2020), 1-13.
26. Aweda, F., Adebayo, S., Samson, T. and Ojedokun, I., "Modelling net radiative measurement of meteorological parameters using merra-2 data in sub-sahara african town", ***Iranian (Iranica) Journal of Energy & Environment***, Vol. 12, No. 2, (2021), 173-180.
27. Bazoobandi, H.J.I.J.o.E., "Wavelet neural network with random wavelet function parameters", ***International Journal of Engineering, Transactions A: Basics***, Vol. 30, No. 10, (2017), 1510-1516, doi: 10.5829/ije.2017.30.10a.12.

Persian Abstract

چکیده

فرکانس رادیویی در عملکرد بهینه سیستم های رادیویی بسیار حیاتی است و یکی از ویژگی هایی است که بر امواج الکترومغناطیسی در تروپوسفر تأثیر می گذارد. این مطالعه مقایسه ای از انواع مختلف شبکه های عصبی بازگشتی را برای پیش بینی ضریب شکست رادیویی ارائه کرد. ضریب شکست رادیویی بر اساس داده‌های اندازه‌شناختی چهل و یک ساله (۱۹۸۰ تا ۲۰۲۰) به‌دست‌آمده از پایگاه داده تحلیل مجدد داده‌های MERRA-2 پیش‌بینی می‌شود. ضریب شکست با استفاده از استاندارد اتحادیه بین المللی مخابرات (ITU) محاسبه شد. ضریب شکست همبستگی به دو دسته قوی، ضعیف و بدون همبستگی طبقه بندی شد. بارندگی، رطوبت نسبی و فشار هوا در دسته اول قرار می گیرند، دما در دسته دوم و سرعت باد در دسته آخر کاهش می یابد. آینده واقعی و مقادیر پیش‌بینی‌شده ضریب شکست رادیویی نزدیک به GRU هستند که بهتر از دو مدل دیگر (LSTM) و (BiLSTM) عمل می‌کنند که دقت مدل پیشنهادی را ثابت می‌کند. در نتیجه، مدل پیشنهادی می‌تواند وضعیت فرکانس رادیویی مکان‌ها را در زمان‌های مختلف فصل ایجاد کند که در طراحی، توسعه و استقرار مؤثر سیستم‌های ارتباط رادیویی از اهمیت بالایی برخوردار است.